

Document downloaded from:

<http://hdl.handle.net/10251/82844>

This paper must be cited as:

Martinez Franco, R.; Paris-Carrizo, CG.; Moliner Marin, M.; Corma Canós, A. (2016).  
Synthesis of highly stable metal-containing extra-large-pore molecular sieves. *Philosophical Transactions A: Mathematical, Physical and Engineering Sciences*. 374(2061).  
doi:10.1098/rsta.2015.0075



The final publication is available at

<http://doi.org/10.1098/rsta.2015.0075>

Copyright Royal Society, The

Additional Information

# Synthesis of highly stable metal-containing extra-large pore molecular sieves

Raquel Martínez-Franco, Cecilia Paris, Manuel Moliner\*, Avelino Corma\*

*Instituto de Tecnología Química, Universidad Politécnica de Valencia - Consejo Superior de Investigaciones Científicas (UPV-CSIC), Valencia, 46022, Spain.*

**Keywords:** Metalloaluminophosphates (MeAlPO), extra-large pore zeotypes, heterogeneous catalysis

---

## Abstract

The isomorphous substitution of two different metals (Mg and Co) within the framework of the ITQ-51 zeotype (IFO structure) using bulky aromatic proton sponges as organic structure-directing agents (OSDAs) has allowed the synthesis of different stable metal-containing extra-large pore zeotypes with high pore accessibility and acidity. These metal-containing extra-large pore zeolites, named MgITQ-51 and CoITQ-51, have been characterized by different techniques, such as PXRD, SEM, EDX, UV-Vis spectroscopy, NH<sub>3</sub>-TPD, and FT-IR spectroscopy, to study their physico-chemical properties. The characterization confirms the preferential insertion of Mg and Co atoms within the crystalline structure of the ITQ-51 zeotype, providing high Brønsted acidity, and allowing their use as efficient heterogeneous acid catalysts in industrially-relevant reactions involving bulky organic molecules.

## 1. - Introduction

One of the main challenges in the field of catalysis is the preparation of highly stable molecular sieves containing extra-large pores (> than 7 Å) with adequate acid properties.<sup>[1]</sup> These type of crystalline microporous materials with large pore accessibility and acidity are highly demanded by industry due to their ability to process bulky reactants and products, while decreasing diffusional limitations of large molecules and increasing the catalyst lifetime by reducing the pore blocking by coke formation.<sup>[2,3]</sup>

Since the discovery of the first extra-large pore aluminophosphate molecular sieve containing 18-ring channels (~10 Å), which was named VPI-5,<sup>[4]</sup> several new phosphate-based molecular sieves with extra-large pores have been described.<sup>[1,2]</sup> Unfortunately, these extra-large pore phosphate-related materials show low hydrothermal stability after being treated under high temperatures in presence of air to remove the organic moieties occluded within the pores.<sup>[1,2]</sup> In these cases, a remarkable loss of crystallinity or even the collapse of the entire crystalline structure is observed after the calcination treatment, precluding their use for catalytic applications. The reason of the low hydrothermal stability of most of these extra-large pore phosphate-related materials comes from the presence of metal mixtures in tetrahedral-octahedral coordination, terminal -OH groups or some non-tetrahedral species (i.e. OH, H<sub>2</sub>O or F).<sup>[1,5]</sup> Therefore, the preparation of stable extra-large pore molecular sieves with larger pores than 14-ring openings is a very challenging issue.

Traditionally, one of the preferred strategies to synthesize zeolites with extra-large pores has been the use of bulky and rigid organic molecules as organic structure directing agents (OSDAs).<sup>[1b]</sup> Having that in mind, we have recently proposed the use of a bulky aromatic proton sponge molecule as OSDA [1,8-bis(dimethylamino)naphthalene, DMAN, see Figure 1],<sup>[6]</sup> since this organic molecule presents the proper physico-chemical properties,<sup>[7]</sup> including the suitable size and rigidity, to direct the crystallization of extra-large pore zeolites. In this sense, the DMAN molecule has allowed the synthesis of a new silicoaluminophosphate (SAPO), named ITQ-51, which presents extra-large 16-ring pores (~9 Å) in its crystalline structure, and even more important, shows very high hydrothermal stability after calcination treatments.<sup>[6]</sup> Up to that moment, only one zeolite, the germanosilicate ITQ-40, was described in the literature containing 16-ring pores in its framework,<sup>[8]</sup> but its structure collapsed after calcination and exposure to ambient conditions. This lack of crystallized zeolites containing 16-ring pores reveals the difficulties of finding appropriate OSDAs able to stabilize this type of channels.<sup>[9]</sup> However, the bulky OSDAs formed by the particular supramolecular self-assembling of two aromatic DMAN molecules in the synthesis media, show the adequate shape and size to stabilize the formation of 16-ring pores by proper host-guest interactions during nucleation and crystallization processes.<sup>[10]</sup>

\*Author for correspondence ([acorma@itq.upv.es](mailto:acorma@itq.upv.es), [mmoliner@itq.upv.es](mailto:mmoliner@itq.upv.es)).

†Present address: Instituto de Tecnología Química, Universidad Politécnica de Valencia - Consejo Superior de Investigaciones Científicas (UPV-CSIC), Valencia 46022, Spain.

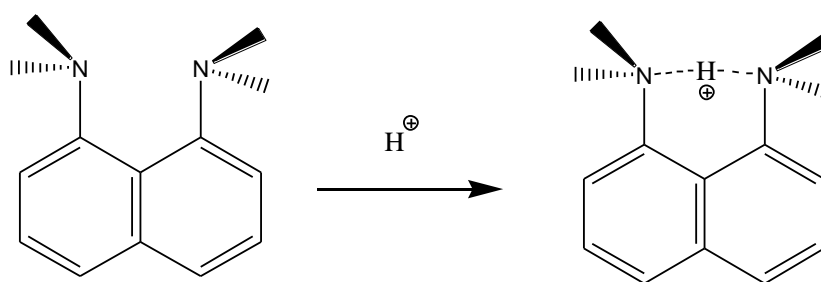


**Figure 1.** Proton sponge 1,8-bis(dimethylamino)naphthalene [DMAN].

Unfortunately, the silicoaluminophosphate form of the ITQ-51 shows low Brønsted acidity because the isomorphous substitution of Si atoms within the SAPO material resulted in the formation of large “silicon islands” in the zeolitic frameworks,<sup>[6]</sup> and it has been broadly described that these silicon-rich areas show very low Brønsted acidity.<sup>[11]</sup> However, other elements, such as transition metals, could also be isomorphically substituted within the neutral AIPO frameworks in addition to silicon atoms, resulting in the formation of MeAIPO materials.<sup>[12]</sup> The selective isomorphous substitution of a divalent metal (Me<sup>2+</sup>) by Al<sup>3+</sup> atoms in framework positions would allow metal-containing AIPO-related materials with different acid and redox properties.<sup>[13]</sup>

Herein, the isomorphous substitution of two different divalent metals (Me = Mg<sup>2+</sup> and Co<sup>2+</sup>) within the framework of the ITQ-51 zeotype (IFO structure) is described. The resultant MeAIPOs materials, MgITQ-51 and CoITQ-51, have been characterized using different techniques, such as powder X-ray diffraction (PXRD), UV-Vis spectroscopy, scanning electron microscopy (SEM), temperature programmed desorption of ammonia (NH<sub>3</sub>-TPD), and FT-IR spectroscopy, to investigate their physico-chemical properties, and to determine the nature of the metal active sites. The metal-containing ITQ-51 zeotypes show high hydrothermal stability and high Brønsted acidity, being attractive materials for their use as heterogeneous acid catalysts in chemical processes requiring the presence of bulky organic molecules.

## 2. – Experimental

### 2.1. - Synthesis of MeITQ-51 materials

In a general procedure for the MeITQ-51 preparation, the required amount of the organic molecule DMAN (99 wt%, Sigma-Aldrich), acting as OSDA, was first mixed with distilled water and the required amount of the orthophosphoric acid (85%wt, Aldrich), keeping this mixture under stirring for 2 h until complete dissolution of the OSDA. Then, a 20%wt aqueous solution of a metal source (magnesium chloride hexahydrate, ≥98wt%, Fluka; or cobalt (II) acetate tetrahydrate, ≥98wt%, Sigma-Aldrich) was also introduced into the synthesis gel, leaving the mixture under stirring for 20 minutes. Finally, the alumina (75%wt, Condea) source was added into the gel, and the mixture was stirred for 30 minutes. The resultant gel was transferred to an autoclave with a Teflon liner, and heated at 150°C under static conditions for five days. **Table 1** summarizes the experimental conditions selected for the synthesis of the different MeITQ-51. Crystalline products were filtered and washed with abundant water, and dried at 100°C overnight. The samples were calcined at 550°C in air to properly remove the occluded organic species.

**Table 1.** Molar ratios selected for the synthesis of the different MeITQ-51

Sample <sup>a</sup>	P/Al	Me/(Al+P)	DMAN/(Al+P)	H <sub>2</sub> O/(Al+P)
MgITQ-51_1	1.05	0.026	0.3	10
MgITQ-51_2	1.11	0.053	0.3	10
CoITQ-51_1	1.05	0.026	0.3	10
CoITQ-51_2	1.11	0.053	0.3	10

<sup>a</sup> All materials were crystallized at 150°C for 5 days

### 2.2. - Characterization

The as-synthesized and calcined samples were characterized by several analytical and spectroscopic techniques. Powder X-ray diffraction (PXRD) measurements were performed with a multisample Philips X'Pert diffractometer equipped with a graphite monochromator, operating at 45 kV and 40 mA, and using Cu K $\alpha$  radiation ( $\lambda = 0,1542$  nm).

The chemical analyses were obtained with the energy dispersive X-ray spectrometry (EDX) with electron excitation at JEOL JSM-6300 scanning electron microscope (SEM). The organic content of as-made materials was determined by elemental analysis performed with a SCHN FISOONS elemental analyzer.

The morphology of the samples was studied by field emission scanning electron microscopy (FESEM) using a ZEISS Ultra-55 microscope.

UV-Vis spectra were obtained with a Perkin-Elmer (Lambda 19) spectrometer equipped with an integrating sphere with BaSO<sub>4</sub> as reference.

NH<sub>3</sub>-TPD experiments were carried out in a Micromeritics 2900 apparatus. A calcined sample (100 mg) was activated by heating to 400°C for 2 h in an oxygen flow and for 2 h in an argon flow. Subsequently, the samples were cooled to 176°C, and NH<sub>3</sub> was adsorbed. The NH<sub>3</sub> desorption was monitored with a quadrupole mass spectrometer (Balzers, Thermo Star GSD 300 T) while the temperature of the sample was ramped at 10°C/min under helium flow. Total ammonia adsorption was measured by repeated injection of calibrated amounts of ammonia at 176°C until saturation. Ammonia desorption was recorded by means of the mass 15, since this mass is less affected by the water desorbed.

Infrared spectra were measured with a Nicolet 710 FT IR spectrometer. Pyridine adsorption-desorption experiments were made on self-supported wafers ( $10 \text{ mg}\cdot\text{cm}^{-1}$ ) of original samples previously activated at  $400^\circ\text{C}$  and  $10^{-2} \text{ Pa}$  for 2 hours. After wafer activation, the base spectrum was recorded and pyridine vapour ( $6.5 \cdot 10^{-2} \text{ Pa}$ ) was admitted in the vacuum IR cell and adsorbed onto the zeolite. Pyridine was desorbed at different temperatures ( $150$ ,  $250$  and  $350^\circ\text{C}$ ) followed by the IR measurement at room temperature. All of the spectra were scaled according to the sample weight

### 3. – Results and Discussion

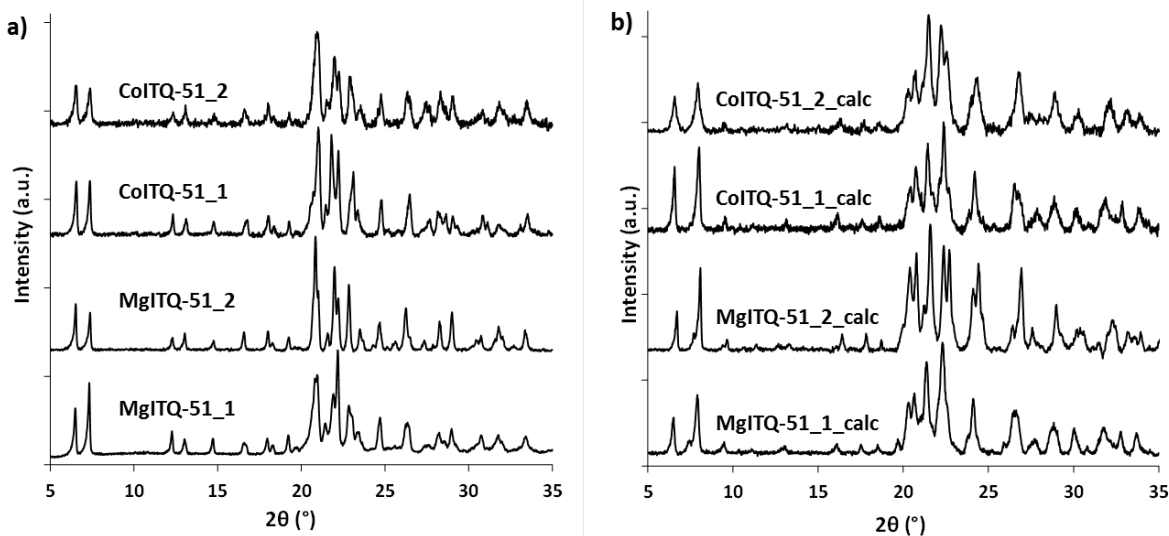
The silicoaluminophosphate (SAPO) form of the ITQ-51 zeotype was synthesized with the following gel composition [ $\text{Si}/(\text{Al}+\text{P})=0.1$ ,  $\text{P}/\text{Al}=0.9$ ,  $\text{DMAN}/(\text{Al}+\text{P})=0.3$ ,  $\text{H}_2\text{O}/(\text{Al}+\text{P})=10$ ,  $T=150^\circ\text{C}$ ] using the bulky aromatic proton sponge DMAN as OSDA.<sup>[6]</sup> This material showed high hydrothermal stability after calcination procedures but, low Brønsted acidity due to the preferential distribution of the silicon species as “silicon islands” instead of isolated Si tetrahedron.<sup>[6]</sup> The synthesis of SAPO materials with isolated Si species within the framework is a very challenging issue, since the  $\text{SiO}_4$  tetrahedral units tend to coordinate with other  $\text{SiO}_4$  tetrahedral units forming these undesired Si-rich areas.<sup>[11]</sup> Thus, specific host-guest organic-inorganic interactions between the OSDA and the crystalline structure are required not only to direct the formation of the desired crystalline structure with a specific framework but, also, to preferentially place the silicon atoms in framework isolated units. Having that in mind, we thought on introducing divalent transition metal ions ( $\text{Mg}^{2+}$  or  $\text{Co}^{2+}$ ) instead of silicon atoms in the synthesis of the ITQ-51 zeotype, in order to favor their distribution as isolated species in tetrahedral coordination. It is expected that the isomorphic substitution of these divalent metal cations by  $\text{Al}^{3+}$  species would create Brønsted acid sites in these materials, making them attractive as acid catalysts.

For this purpose, the synthesis of the Me-containing ITQ-51 materials has been attempted under similar synthesis conditions to the previously used for the synthesis of the SAPO ITQ-51, and two different molar ratios of the metals [ $\text{Me}/(\text{Al}+\text{P})=0.026$ ,  $0.053$ ] have been studied at  $150^\circ\text{C}$  for 5 days under static conditions. The synthesis conditions of the MeITQ-51 molecular sieves are summarized in **Table 1**.

The PXRD patterns of the as-prepared samples confirm the selective crystallization of the IFO structure for these MeITQ-51 materials (see **Figure 2a**). Interestingly, these metal-containing ITQ-51 materials remain stable after being calcined in air at  $550^\circ\text{C}$  regardless the metal-type and metal-loading introduced (see **Figure 2b** and **Table 1**), revealing the high hydrothermal stability of these calcined extra-large pore zeotypes. It is important to note that after similar calcination processes, most of the reported extra-large pore AIPO-based materials were shown to be unstable.<sup>[1,2]</sup>

**Figure 2.** PXRD patterns of MeITQ-51 materials in their as-prepared (a) and calcined (b) forms.

The MgITQ-51 and CoITQ-51 samples have been characterized by  $\text{N}_2$  adsorption to study their pore accessibility after the calcination treatments at  $550^\circ\text{C}$ . As it can be seen in **Table 2**, the micropore volume achieved for these two calcined materials is



comparable to the micropore volume reported for the original ITQ-51 material in its SAPO form.<sup>[6]</sup>

**Table 2.** Molar ratios selected for the synthesis of the different MeITQ-51

Sample	BET surface area ( $\text{m}^2/\text{g}$ )	Micropore area ( $\text{m}^2/\text{g}$ )	Micropore volume ( $\text{cm}^3/\text{g}$ )
ITQ-51	367	290	0.14
MgITQ51_1	359	319	0.16

The crystal morphology of these Me-containing ITQ-51 materials has been studied by scanning electron microscopy (SEM, see **Figure 3**). These SEM images show a homogeneous crystal distribution for all materials, confirming the absence of amorphous phase or crystalline impurities. The Mg-containing ITQ-51 samples show plate-like crystal morphologies with different crystal size depending on the metal-content (see **Figures 3a** and **3b**). Indeed, the MgITQ-51 sample synthesized with a theoretical Mg/TO<sub>2</sub> molar ratio of 0.026 (see Mg-ITQ51\_1 in **Table 1**) results in larger plate-like crystals (~5-10  $\mu\text{m}$ , see **Figure 3a**), while the MgITQ-51 sample synthesized with a theoretical Mg/TO<sub>2</sub> molar ratio of 0.053 (see Mg-ITQ51\_2 in **Table 1**) shows the formation of smaller plate-like crystals (~2-3  $\mu\text{m}$ , see **Figure 3b**). On the other hand, Co-containing ITQ-51 materials are mainly formed by the aggregation of needle-like crystals, and their size also depends on the metal-content (see **Figures 3c** and **3d**). In this sense, the Co-containing ITQ-51 synthesized with a theoretical Co/TO<sub>2</sub> molar ratio of 0.026 (see Co-ITQ51\_1 in **Table 1**) crystallizes in the form of needles with a length of ~3-5  $\mu\text{m}$  (see **Figures 3c**), while the CoITQ-51 sample synthesized with a theoretical Co/TO<sub>2</sub> molar ratio of 0.053 (see Co-ITQ51\_2 in **Table 1**) shows the aggregation of needle-like crystals of ~1  $\mu\text{m}$  (see **Figure 3d**).

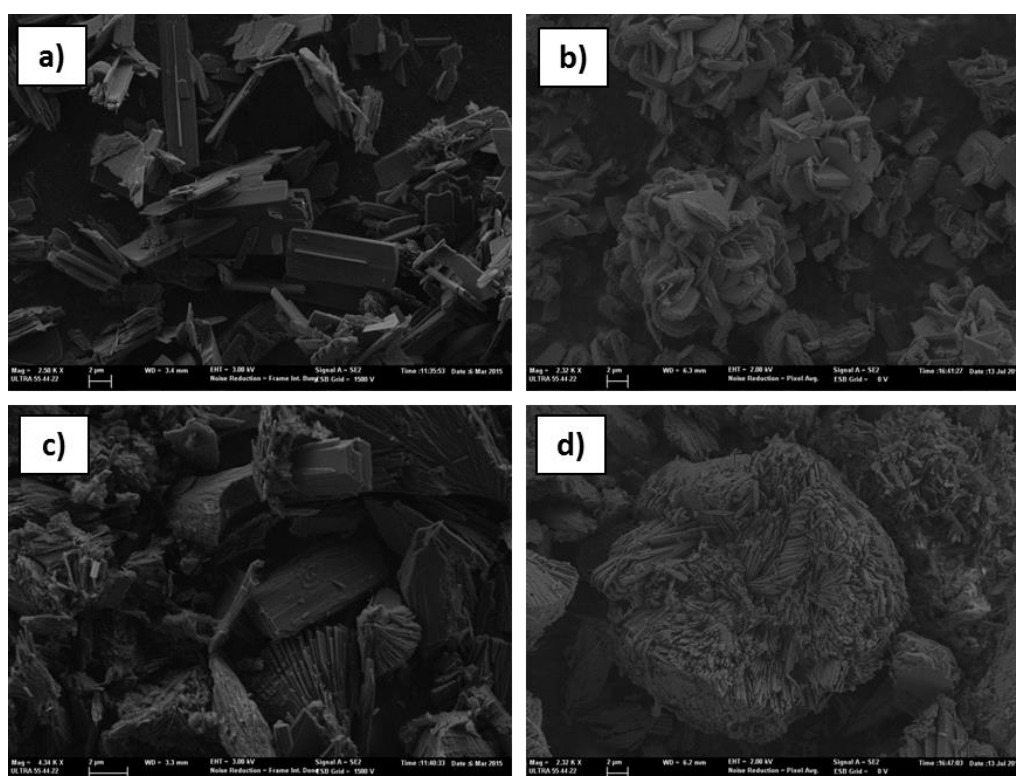


**Figure 3.** SEM images of MgITQ-51\_1 (a), MgITQ-51\_2 (b), CoITQ-51\_1 (c) and CoITQ-51\_2 (d)

Elemental analyses of the as-prepared Me-containing ITQ-51 materials show a C/N molar ratio close to 7 (see C/N ratios in **Table 3**). Taking into account that the theoretical C/N ratio of the DMAN molecule is 7 (see **Figure 1**), the elemental analyses indicate that most of the proton sponge DMAN molecules entrapped within the pores of the ITQ-51 zeotypes remain intact after the crystallization processes.

**Table 3.** Chemical and elemental analysis of the as-prepared MeITQ-51 zeotypes

Sample	Me <sup>a</sup>	Al <sup>a</sup>	P <sup>a</sup>	Me/(Al+P)	(Me+Al)	%wt N	%wt C	C/N <sub>real</sub>
MgITQ-51_1	0.025	0.46	0.51	0.026	0.49	2.53	14.89	6.9
MgITQ-51_2	0.059	0.45	0.49	0.059	0.51	N.D. <sup>b</sup>	N.D. <sup>b</sup>	N.D. <sup>b</sup>
CoITQ-51_1	0.034	0.44	0.52	0.035	0.48	2.63	14.88	6.6
CoITQ-51_2	0.053	0.42	0.52	0.056	0.48	2.13	12.72	6.7

<sup>a</sup> Normalized mole fractions; <sup>b</sup> N.D.: Non-determined

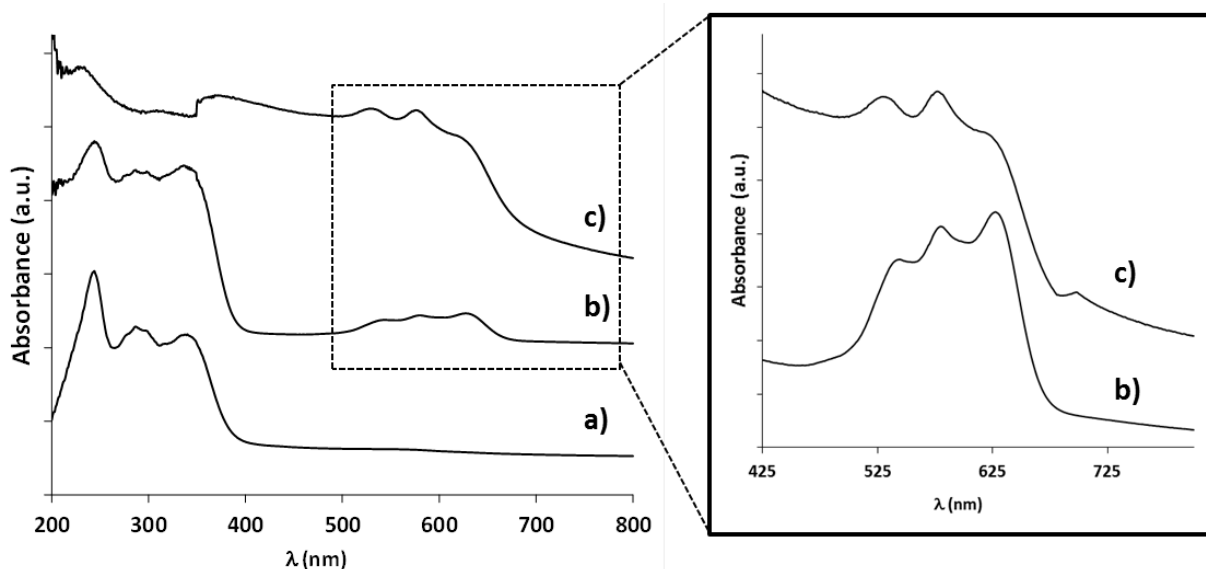
In order to determine the real metal content in the Me-containing ITQ-51 materials, the samples have been characterized by energy dispersive X-ray spectrometry (EDX) with electron excitation, using a scanning electron microscope (SEM). As it can be

seen in **Table 3** the final Me/TO<sub>2</sub> molar ratios are very similar to the theoretical molar ratios introduced in the synthesis gels (see **Table 1**). Interestingly, the (Me+Al) molar fractions are quite close to the molar fraction of phosphorous (~0.5), suggesting that both metals, Mg and Co, are able to undergo the selective isomorphous substitution of aluminum in framework positions during the synthesis of the MeITQ-51 materials. If this is so, it could be expected the presence of Brønsted acid sites in the calcined MeITQ-51 samples.

The incorporation of cobalt ions within the crystalline framework of CoAlPO materials has been characterized in the literature using UV-Vis spectroscopy.<sup>[14]</sup> Therefore, the as-prepared and calcined CoITQ51\_2 samples have been studied by UV-Vis spectroscopy to see if the cobalt ions have been properly inserted within the crystalline structure of the ITQ-51. On one hand, the UV-Vis spectrum of the as-prepared CoITQ-51\_2 zeotype in the UV region shows the appearance of three absorption signals between 200 and 400 nm (see **Figure 4b**). However, these signals cannot be assigned to framework or extra-framework metallic species, since similar bands are also observed in the UV-Vis spectrum of the as-prepared Co-free ITQ-51 in its silicoaluminophosphate form (see **Figure 4a**). Thus, these bands may be attributed to the presence of entrapped DMAN molecules within the pores of the as-prepared CoITQ-51\_2 material. Interestingly, the UV-Vis spectrum of the as-prepared CoITQ-51\_2 zeotype also shows the presence of three absorbance bands in the visible region centered at 540, 580 and 625 nm (see **Figure 4b-inset**). These signals are characteristic of Co(II) species in crystalline tetrahedral environments,<sup>[15]</sup> indicating that most of the cobalt species have been incorporated into the ITQ-51 framework. On the other hand, upon calcination of CoITQ-51\_2 at 550°C in presence of air, a new and weak adsorption band appeared around 400 nm (see **Figure 4c**), in addition to the three absorbance bands between 500 and 625 nm (see **Figure 4c-inset**). This new adsorption band could be assigned to trivalent cobalt [Co(III)] species in framework positions, formed by oxidation of part of the divalent cobalt species [Co(II)] during the calcination process.<sup>[16]</sup>

**Figure 4.** UV-Vis spectra of the as-prepared ITQ-51 in its SAPO form (a), as-prepared CoITQ-51\_2 (b), and calcined CoITQ-51\_2 (c).

The acidity of these metal-containing ITQ-51 samples has been characterized by temperature-programmed desorption of ammonia (NH<sub>3</sub>-TPD) and also by in situ infrared spectroscopy of pyridine adsorption/desorption. NH<sub>3</sub>-TPD clearly shows the presence of at least two well-defined NH<sub>3</sub>-desorption peaks for the MeITQ-51 materials (see **Figure 5**). The first peak centered at 200°C is attributed to the presence of weak acid sites (physisorbed ammonia or terminal P-OH groups),<sup>[17]</sup> while the second peak centered at 330°C is attributed to the presence of strong acid sites.<sup>[18]</sup> The concentration of weak and strong acid sites can be quantified from NH<sub>3</sub>-TPD experiments by proper deconvolution of the curves (see **Figure 5** and **Table 4**). As seen in **Table 4**, the amount of strong acid sites for MgITQ-51\_2 sample is much higher than for MgITQ-51\_1 sample, in clear relationship with the



highest Mg loading in the MgITQ-51\_2 sample (see **Table 3**). In contrast, the strength of the acid sites presents in MgITQ-51\_2 and CoITQ-51\_2 samples are quite similar (see **Table 4**), and this comparable acidity could be attributed to their analogous metal content (Mg and Co, see **Table 3**). The good correlation between the acid strength and the metal content in the final MeITQ-51 samples suggests that most of the Co and Mg species, must be placed in tetrahedral coordination within the zeolitic framework, and consequently, leading to the formation of Brønsted acid sites by isomorphous substitution of aluminum atoms.

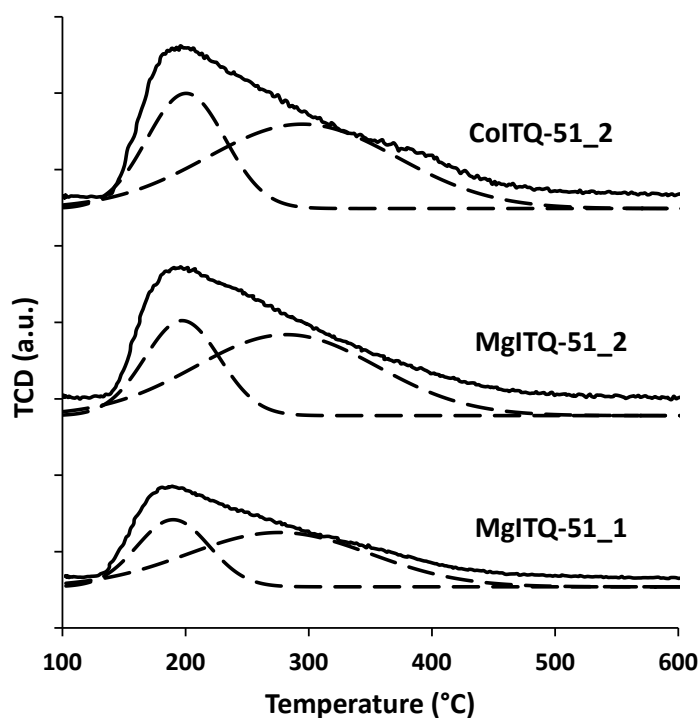


**Figure 5.** Temperature-programmed desorption of ammonia of the calcined MeITQ-51 materials

**Table 4.** Acid strength of the calcined MgITQ-51 and CoITQ-51 molecular sieves calculated from NH<sub>3</sub>-TPD

Sample	Acidity concentration (mmol NH <sub>3</sub> /g)	
	Weak	Strong
MgITQ-51_1	0.113	0.231
MgITQ-51_2	0.318	0.657
CoITQ-51_2	0.285	0.509

Finally, the calcined MgITQ-51\_2 and CoITQ-51\_2 samples, containing a similar metal loading (see **Table 3**), have been characterized by in situ infrared spectroscopy of pyridine adsorption/desorption. The FTIR spectra of adsorbed pyridine after desorption treatments at 150, 250, and 350°C are represented in **Figure 6**. After the desorption treatment at 150°C, both samples show the characteristic IR band of the pyridinium ion at 1545 cm<sup>-1</sup>, which is associated with the presence of Brønsted acids sites. Interestingly, the calcined MgITQ-51\_2 and CoITQ-51\_2 samples mostly retain the IR band of the pyridinium ion after increasing the pyridine desorption temperature at 250°C (see **Figure 6**), revealing a medium-strong Brønsted acid behaviour. These results are in agreement with the results obtained by temperature-programmed desorption of ammonia.

The catalytic activity of the different hydrothermally-stable metal-containing ITQ-51 materials synthesized along the present work with different acid strength will be evaluated for different industrially relevant chemical processes involving the presence of bulky organic molecules.

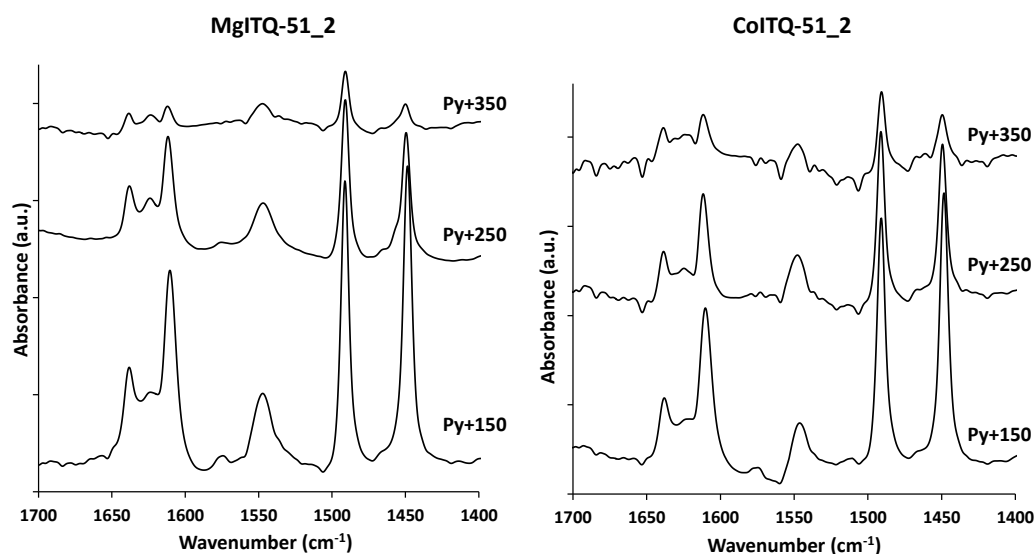


**Figure 6.** FTIR spectra of pyridine adsorption/desorption on MgITQ-51\_2 and CoITQ-51\_2 molecular sieves

#### 4. – Conclusions

The synthesis of the extra-large pore metal-containing ITQ-51 zeotypes, as MgITQ-51 and CoITQ-51, with different and controlled metal-loadings has been achieved by using a bulky aromatic proton sponge, DMAN, as OSDA.

The synthesized materials have been characterized in detail, demonstrating that Mg and Co metals have been mainly incorporated into the ITQ-51 framework by the isomorphic substitution of these divalent metals ( $Mg^{2+}$  or  $Co^{2+}$ ) by  $Al^{3+}$  atoms. Moreover, these metal-containing ITQ-51 materials show excellent hydrothermal stabilities after calcination treatments at 550°C.

Finally, temperature-programmed desorption of ammonia ( $NH_3$ -TPD) and in-situ infrared spectroscopy of pyridine adsorption/desorption demonstrate that the insertion of these divalent metals in the ITQ-51 crystalline structure, results in the generation of medium-strong Brønsted acid sites, potentially allowing their use as acid heterogeneous catalysts in future catalytic studies.

#### Acknowledgments

Financial support by the Spanish Government-MINECO through “Severo Ochoa” (SEV 2012-0267), Consolider Ingenio 2010-Multicat, and MAT2012-37160 is acknowledged.

#### References

1. a) Jiang J, Yu J, Corma A. 2010. Extra-Large-Pore Zeolites: Bridging the Gap between Micro and Mesoporous Structures. *Angew. Chem., Int. Ed.* 49, 3120–3145. (doi: 10.1002/anie.200904016); b) Moliner M, Rey F, Corma A. 2013. Towards the rational design of efficient organic structure-directing agents for zeolite synthesis. *Angew. Chem. Int. Ed.* 52, 13880–13889. (doi: 10.1002/anie.201304713); c) Davis ME. 1997. The Quest for Extra-large Pore, Crystalline Molecular sieves. *Chem. Eur. J.* 3, 1745–1750. (doi: 10.1002/chem.19970031104).
2. a) Davis ME. 2002. Ordered porous materials for emerging applications. *Nature* 417, 813–821. (doi:10.1038/nature00785); b) Corma A. 2003. State of the art and future challenges of zeolites as catalysts. *J. Catal.* 216, 298–312. (doi:10.1016/S0021-9517(02)00132-X).
3. Corma A, Diaz-Cabañas M, Jordá JL, Martínez C, Moliner M. 2006. High-throughput synthesis and catalytic properties of a molecular sieve with 18- and 10-member rings. *Nature*. 443, 842–845. (doi:10.1038/nature05238).
4. Davis ME, Saldarriaga C, Montes C, Garces J, Crowder C. 1988. A molecular sieve with Eighteen - membered Rings. *Nature*. 331, 698–699. (doi: 10.1038/331698a0).
5. Corma A, Davis ME. 2004. Issues in the synthesis of crystalline Molecular sieves: Towards the Crystallization of Low Framework-Density Structures. *ChemPhysChem*. 5, 304–313. (doi: 10.1002/cphc.200300997).
6. Martínez-Franco R, Moliner M, Yun Y, Sun J, Wan W, Zou X, Corma A. 2013. Synthesis of an extra-large molecular sieve using proton sponges as organic structure-directing agents. *Proc. Natl. Acad. Sci. USA* 110, 3749–3754. (doi:10.1073/pnas.1220733110).
7. Staab HA, Saupe T. 1988. “Proton Sponges” and the Geometry of Hydrogen Bonds: Aromatic Nitrogen Bases with Exceptional Basicities. *Angew. Chem., Int. Ed.* 27, 865–879. (doi:10.1002/anie.198808653).
8. Corma A, Díaz-Cabañas MJ, Jiang J, Afeworki M, Dorset DL, Soled SL, Strohmaier KG. 2010. Extra-large pore zeolite (ITQ-40) with the lowest framework density containing double four- and double three-rings. *Proc. Natl. Acad. Sci. USA* 107, 13997–14002. (doi: 10.1073/pnas.1003009107).
9. Curtis RA, Deem MW. 2003. A statistical mechanics study of ring size, ring shape, and the relation to pores found in zeolites. *J.*

---

Phys. Chem. B. 107, 8612-8620. (doi: 10.1021/jp027447+).

10. Martínez-Franco R, Sun J, Sastre G, Yun Y, Zou X, Moliner M, Corma A. 2014. Supra-molecular assembly of aromatic proton sponges to direct the crystallization of extra-large-pore zeotypes. *Proc. R. Soc. A.* 470, 20140107. (doi: 10.1098/rspa.2014.0107).
11. Man PP, Briend M, Peltre MJ, Lamy A, Beaunier P, Barthomeuf D. 1991. A topological model for the silicon incorporation in SAPO-37 molecular sieves: Correlations with acidity and catalysis. *Zeolites.* 11, 563-572. (doi: 10.1016/S0144-2449(05)80006-5).
12. Wilson ST, Flanigen EM. 1986. Crystalline metal aluminophosphates, U.S. Patent 4,567,029.
13. a) Corà F, Saadouni I, Richard C, Catlow A. 2002. Lewis Acidity in Transition-Metal-Doped Microporous Aluminophosphates. *Angew. Chem., Int. Ed.* 41, 4677-4680 (doi:10.1002/anie.200290013); b) Hartmann M, Kevan L. 2002. Substitution of transition metal ions into aluminophosphates and silicoaluminophosphates: characterization and relation to catalysis. *Res. Chem. Intermed.* 28, 625-695. (doi: 10.1163/15685670260469357).
14. Šponer J, Čejka J, Dědeček J, Wichterlová B. 2000. Coordination and properties of cobalt in the molecular sieves CoAPO-5 and -11. *Micropor. Mesopor. Mater.* 37, 117-127. (doi:10.1016/S1387-1811(99)00258-9).
15. Singh PS, Shaikh RA, Bandyopadhyay R, Rao BS. 1995. Synthesis of CoVPI-5 with bifunctional catalytic activity. *J. Chem. Soc. Chem. Commun.* 2255-2256. (doi: 10.1039/C39950002255); b) Jhung SH, Jin T, Kim YH, Chang JS. 2008. Phase-selective crystallization of cobalt-incorporated aluminophosphate molecular sieves with large pore by microwave irradiation. *Micropor. Mesopor. Mater.* 109, 58-65. (doi 10.1016/j.micromeso.2007.04.031).
16. Iton LE, Choi I, Desjardins JA, Maroni VA. 1989. Stabilization of Co (III) in aluminophosphate molecular sieve frameworks. *Zeolites* 9, 535-538. (doi:10.1016/0144-2449(89)90051-1); b) Frache A, Gianotti E, Marchese L. 2003. Spectroscopic characterisation of microporous aluminophosphate materials with potential application in environmental catalysis. *Catal. Today.* 77, 371-384. (doi :10.1016/S0920-5861(02)00381-4).
17. Yu T, Wang J, Shen M, Li W. 2013. NH<sub>3</sub>-SCR over Cu/SAPO-34 catalysts with various acid contents and low Cu loading. *Catal. Sci. Technol.* 2013, 3234-3241. (doi:10.1039/C3CY00453H).
18. Yang X, Ma H, Xua Z, Xu Y, Tian Z, Lin L. 2007. Hydroisomerization of n-dodecane over Pt/MeAPO-11 (Me = Mg, Mn, Co or Zn) catalysts. *Catal. Commun.* 8, 11232-1238. (doi: doi:10.1016/j.catcom.2006.11.005).